

Biological Behavior of Osteoblast-like Cells on Titania and Zirconia Films Deposited by Cathodic Arc Deposition

Shailin Zhang · Junying Sun · Ying Xu ·
Shi Qian · Bing Wang · Fei Liu · Xuanyong Liu

Received: 5 July 2012 / Accepted: 19 September 2012 / Published online: 2 October 2012
© The Author(s) 2012. This article is published with open access at Springerlink.com

Abstract Cathodic arc deposition technique was used to deposit zirconia (ZrO_2) films and titania (TiO_2) films on titanium (Ti) disks respectively. The surface topography was characterized by scanning electron microscopy and atomic force microscopy. The element composition of the films was detected by X-ray photoelectron spectroscopy. The phase of films was identified by thin film X-ray diffraction. The biological behavior of osteoblast-like MG63 cells cultured on Ti, TiO_2 and ZrO_2 was investigated and the possible signaling molecules involved was studied by the gene expressions of integrin $\beta 1$, extracellular related kinase 1/2 (ERK1/2), and *c-fos*. The results indicated that both the TiO_2 and ZrO_2 films were amorphous. Scanning electron microscopy study showed that the adhesion of MG63 cells on TiO_2 and ZrO_2 films was significantly enhanced compared to Ti. The CCK8 assay indicated that the TiO_2 and ZrO_2 films promoted the proliferation of MG-63 cells. The alkaline phosphatase (ALP) activity test and the production of type collagen I (COLI) by immunofluorescence showed that both the TiO_2 and ZrO_2 films can enhance ALP activity and COLI expression of MG-63 cells. In addition, the ALP activity on ZrO_2 films was higher than on TiO_2 films at day 4, which indicate ZrO_2

films may lead to promotion of a more osteoblastic phenotype of MG-63 cells than TiO_2 films. Real-time polymerase chain reaction analysis demonstrated that The gene expression of integrin $\beta 1$, ERK1/2, and *c-fos* was higher on TiO_2 and ZrO_2 films than on Ti. The present work suggests that the amorphous ZrO_2 films produced by cathodic arc deposition may be favorable for orthopedic implant applications and worth further study.

1 Introduction

The prolonged lifespan and greater expectation towards the quality of life have lead to an increase in the number of artificial joint replacement. Titanium (Ti) and its alloys are currently the most widely used materials as a component of articular prosthesis due to their excellent biocompatibility, good chemical stability and superior mechanical properties. The clinical success of an implant is strongly affected by the process of direct apposition of bone tissue to the implanted material, which is known as osseointegration [1]. In the past few decades, a number of techniques based on surface modification aimed at improving the biocompatibility and osseointegration of Ti-based implants have been suggested [2–8].

Depositing a bioactive coating on orthopedic implants is an attractive method that is of great interest for biomedical applications since it can retain the key bulk properties of the material while modifying the surface to improve osseointegration and biocompatibility. However, the main drawbacks of these coatings are their low bonding strength and poor chemical stability, which will result in delamination and degradation of the coatings and lead to implant failure eventually. Thus, modifying the implant with bioactive thin films may be an attractive method, because such

S. Zhang · J. Sun (✉) · B. Wang · F. Liu
Department of Orthopaedics, The First Affiliated Hospital
of Soochow University, 188 Shizi Street, Suzhou 215006,
Jiangsu, China
e-mail: sunjy.suda@hotmail.com

Y. Xu · S. Qian · X. Liu (✉)
State Key Laboratory of High Performance Ceramics
and Superfine Microstructure, Shanghai Institute of Ceramics,
Chinese Academy of Sciences, 1295 Dingxi Road,
Shanghai 200050, China
e-mail: xyliu@mail.sic.ac.cn

thin films may provide close contact of the implant with bone after coating dissolution, which would avoid an interphase between the bone and implant substrate, possibly improving the osseointegration of the implant. Various techniques can be used for preparing thin films on Ti and its alloys. Among them, plasma-assisted filtered cathodic arc deposition (FCAD) is characterized by a very high percentage of vapour ionization, the emission of ions that are multiply charged, and the high kinetic energy of the emitted ions, which can produce good quality films that are structurally uniform, dense and adherent to the substrate [9, 10]. The plasma environment can generate a wide range of subnanosized building units [11] and the electromagnetic and mechanical filtering techniques can remove unwanted macroparticles and neutral atoms. Thus, the filtered cathodic arc deposition turn out to be a very efficient method for synthesis and processing of advanced nanostructured films [12].

TiO₂ coatings have been shown to enhance biocompatibility and bioactivity of the Ti and its alloys [13–17]. Amin et al. [18] deposited TiO₂ thin films onto silicon substrates using filtered cathodic arc deposition, and the TiO₂ thin films can induce carbonated apatite to form on the surfaces in simulated body fluid.

During the past few decades zirconia (ZrO₂) ceramics have increasingly attracted attention on account of its remarkable properties such as good chemical and thermal stability, mechanical properties, high corrosion resistance, and good biocompatibility. ZrO₂ coatings and films for biomedical application have also attracted much attention. It was reported that ZrO₂ films fabricated by micro arc oxidation [19] and plasma spraying [20] were bioactive in vitro, and ZrO₂ coating prepared by dip coating in colloidal suspension can improve dental implant osteointegration in vivo in rabbits [21].

ZrO₂ thin films deposited on Si wafers using plasma-assisted cathodic arc deposition has also been proved to be bioactive and cytocompatible [22]. But ZrO₂ films deposited by cathodic arc deposition for surface modification of Ti substrates are rarely reported. Whether the biocompatibility and bioactivity of ZrO₂ films prepared by cathodic arc deposition are better than that of TiO₂ films is unknown.

Cell signaling affects cell adhesion, proliferation and differentiation. To understand osteoblast responses to the implant material, it is important to understand the cell signaling pathways induced by osteoblast-implant interactions. However, the molecular mechanisms leading to osteoblast behavior on cathodic arc deposited ZrO₂ films and TiO₂ films are not fully understood.

Integrins are transmembrane receptors which bind the cell to extracellular matrix (ECM) and elicit signals that are transmitted into the cell [23]. The integrin-ECM interaction activates the mitogen-activated protein kinase (MAPK)

signal transduction pathway and other various intracellular signaling cascades, which play a pivotal role in mediating osteoblast activity [24, 25].

In this work, ZrO₂ and TiO₂ films were respectively deposited onto Ti disks by filter cathodic arc deposition. The adhesion, proliferation and differentiation of osteoblasts on ZrO₂ films and TiO₂ films were systematically studied and compared. Then we studied the gene expression of possible signaling molecules involved in the MAPK/ERK pathway.

2 Materials and Methods

2.1 Material Preparation

Two kinds of titanium disks (diameter = 5.8 and 31 mm respectively, thickness = 3 mm) were obtained from pure commercial titanium. The Ti disks were mechanically polished and cleaned in acetone, alcohol, and deionized water in sequence and dried in air.

The as-deposited films were fabricated in the laboratory of Shanghai Institute of Ceramics using a filtered cathodic arc system [22]. The samples were processed with deposition using filtered Ti cathodic arc plasma sources for TiO₂ films and Zr cathodic arc plasma sources for ZrO₂ films in oxygen atmosphere. In deposition, the pulse duration of cathodic current was 2,000 μs and the frequency was 70 Hz. The direct current voltage of 50 V and a bias of -450 V were superimposed to the sample during deposition. The working pressure was 9×10^{-3} Pa and the deposition time was 60 min. After the deposition treatment, the samples were washed with deionized water and dried in air.

The surface morphology of the films was observed by scanning electron microscopy (SEM, FEI-QUANTA 200-FEG, FEI, American) and atomic force microscopy (AFM, SPI3800N, SEIKO, Japan) (The surface of the titanium disks used as the substrate of the films was too rough to meet the demand of AFM observation. So we deposited TiO₂ and ZrO₂ films on silicon wafers instead for AFM observation.). The phase of films was identified by thin film X-ray diffraction (TF-XRD, D/MAX-2550, Rigaku, Japan) using a Cu K α radiation source (1.5148 Å) at 40 kV and 100 mA with a glancing angle fixed at 1°. The elemental composition of the films was determined using x-ray photoelectron spectroscopy (XPS, MicroLab 310-F) with monochromatic Al K α radiation.

2.2 In Vitro Cell Culture

Human osteosarcoma cell line MG63 was used in this work. MG-63 cells were cultured in DMEM medium

(supplemented with 10 % fetal calf serum, FCS, Eurobio) at 37 °C in a moist 5 % CO₂ atmosphere. The culture medium was replaced every 3 days. After reaching confluence, the cells were released by a trypsin–EDTA solution (0.5 g/L trypsin and 0.2 g/L EDTA, Gibco) and transferred into a new tissue culture flask.

2.3 Cell Morphology

Samples with 5.8 mm in diameter were placed in 96-well plates. 5×10^3 cells were seeded on each sample and cultured under standard cell culture condition for 24 h. Then samples were washed with Phosphate buffer saline (PBS) and fixed with 2.5 % glutaraldehyde buffered by PBS for 2 h at room temperature (RT). They were then successively dehydrated in graded alcohols (30, 50, 70, 90, and 100 %), critical point-dried, sputter-coated with gold and examined using SEM (SL-30, Philips, Holland).

2.4 Counting Kit-8 Assay

Cell proliferation was assessed using a Cell Counting Kit-8 (CCK-8, Dojindo, Japan). Samples with 5.8 mm in diameter were placed in 96-well plates. 1×10^4 cells were dispensed on each sample and incubated for 1, 4, 7, 10 days. At predetermined time points, samples were washed three times with PBS to eliminate non-viable cells. The cells on the samples were incubated with 10 µl of CCK-8 solution for 3 h in the incubator. Then the optical density was measured using a microplate reader at a wavelength of 450 nm. Three samples were tested in each group for each incubation time and the resulting absorbance for each of the samples was averaged. The experiment was run in triplicate.

2.5 Alkaline Phosphatase Activity Assay

Alkaline phosphates (ALP) activity assay was carried out from the culture supernatant. Cells were cultured on ZrO₂ and TiO₂ thin films as well as Ti disks as mentioned in cell proliferation assay. After incubated for 1, 4, 7 and 10 days, the supernatant was collected and assayed for ALP activity immediately using a commercial kit (Jiancheng Technology, Nanjing, China) according to the manufacturer's instructions. Three samples were tested in each group for each incubation time and the ALP activity for each of the samples was averaged. The experiment was run in triplicate.

2.6 Type I Collagen Fluorescence Immunostain

Samples with 5.8 mm in diameter were placed in 96-well plates. 5×10^3 cells were seeded on each sample and cultured under standard cell culture condition for 4 days.

The cells were fixed with 4 % paraformaldehyde for 10 min, washed three times with PBS, permeabilized with 0.1 % Triton X-100 for 5 min and blocked with blocking solution (1 % bovine serum albumin in PBS) for 60 min at RT. The cells were subsequently incubated with polyclonal rabbit anti-collagen I antibody (Novus, USA) for 12 h and washed with PBS. Then the cells were labeled with FITC conjugated goat-anti-rabbit IgG antibody (Bioworld technology, USA) for 1 h. The nucleus was counterstained with DAPI (Molecular Probes, Invitrogen, USA) for 5 min. Immunostained cells were visualized using fluorescence microscope (Axiovert 40 CFL, Zeiss, German). 6 immunofluorescence images for each group were analyzed by Image-Pro Plus 6.0 software (IPP, Media Cybernetics Inc., Silver Spring, MD). The green channel (FITC stain for COLI) was measured and the measurement parameters included area and IOD (integrated optical density). COLI expression was quantified by mean density (mean staining intensity = IOD sum/area sum).

2.7 Real-time Polymerase Chain Reaction (PCR) Analysis

Samples with 31 mm in diameter were placed in 96-well plates. 2.5×10^5 cells were dispensed on each sample and cultured for 6, 24 h and 4, 7 days. The cells on each disk were lysed using Trizol Reagent (Invitrogen, USA) and lysates were collected by pipetting and centrifugation. Total cellular RNA was isolated using Trizol Reagent according to the manufacturer's instruction and collected by ethanol precipitation. Total RNA was quantified using UV spectrophotometry (Beckman DU-600).

First-strand complementary DNA (cDNA) was generated from each total RNA sample using an Invitrogen Superscript First-strand Synthesis system in a standard 20 µl reaction, then was amplified to generate products corresponding to mRNA encoding integrin $\beta 1$, extracellular related kinase 1/2 (ERK1/2), and *c-fos*. Glyceraldehyde-3-phosphate dehydrogenase (GAPDH) was used as the housekeeping gene. The oligonucleotide primers used in the amplification reaction were 5'-GCGCGTGCAGGTGCAATGAAG-3' and 5'-TG TCCGCAGACGCACTCTCC-3' for integrin $\beta 1$; 5'-GGC CGAGGAGCCCCTTACCT-3' and 5'-CACTCCGGGCT GGAAGCGTG-3' for ERK1; 5'-AACAGGCTCTGGCCC ACCCA-3' and 5'-ATGGTGCTTCGGCGATGGGC-3' for ERK2; 5'-CTGTGGCCCCATCGCAGACC-3' and 5'-CG CTCGGCCTCTGTGCATGG-3' for *c-fos*; 5'-ACCACAGT CCATGCCATCAC-3' and 5'-TCCACCACCCTGTTGCT GTA-3' for GAPDH. Real-time PCR was performed using Maxima SYBR Green qPCR Master Mix (Fermentas, Canada) in a real-time PCR System (Applied Biosystems 7500, Bioscience Corporation, USA). Relative mRNA abundance was determined by the $2^{-\Delta\Delta Ct}$ method and reported

as-fold induction. GAPDH abundance was used for normalization. Experiments were performed independently in triplicate.

2.8 Statistical Analysis

The data were expressed as mean \pm standard deviation for all experiments. One way ANOVA and multiple comparison tests were performed to evaluate differences among groups. A p value < 0.05 was considered statistically significant.

3 Results

3.1 Surface Characterizations of the Samples

Figure 1 shows SEM view images of Ti disks (Fig. 1a), TiO₂ (Fig. 1b), and ZrO₂ (Fig. 1c) films. The surface of Ti disks displayed smooth morphology with a few micro pores and grooves. The deposited TiO₂ and ZrO₂ films seem to be uniform, dense and smooth. There was no significant difference in surface morphology between TiO₂ and ZrO₂ films.

Figure 2 shows the AFM views of TiO₂ and ZrO₂ films deposited on silicon wafers. The result indicates that both the TiO₂ and ZrO₂ films deposited by filtered cathodic arc deposition have a nanostructured surface. The Ra values of TiO₂ and ZrO₂ films are 0.054 and 0.256 nm, respectively.

Figure 3 shows the full range XPS spectra (0–1,200 eV) analysis of the TiO₂ (a) and ZrO₂ (b) films. We can see that C1s, O1s, Ti2p, Ti3p and Ti3s peaks are observed in XPS spectra of TiO₂ films, while C1s, O1s, Ti3p, Zr3d, Zr3p, Zr3s, and Zr4s peaks are observed in XPS spectra of ZrO₂ films. The results may indicate that the TiO₂ and ZrO₂ films are respectively distributed on the Ti disks.

Figure 4 shows the thin film XRD patterns of the TiO₂ and ZrO₂ films. No TiO₂ and ZrO₂ peaks were found,

indicating that both the TiO₂ and ZrO₂ films were amorphous. The diffraction peaks of titanium substrate were clearly observed for both TiO₂ and ZrO₂ films.

3.2 Morphology of Osteoblasts

Figure 5 shows the morphologies of osteoblastic cells attached on titanium disks (a, d), titania films (b, e) and zirconia films (c, f) for 24 h at 200 \times (a, b, c) and 2,000 \times (d, e, f) magnification. After cultured for 24 h, cells on Ti disks were sparse and displayed round or elongated morphology. However, cells on TiO₂ and ZrO₂ films showed polygonal shaped and appeared more spreading and flattened than on Ti disks. Cellular edge extended larger lamellipodia and longer filopodia from cellular edge than on Ti disks. No obvious difference in cell morphology was observed between osteoblasts on TiO₂ and ZrO₂ films.

3.3 CCK-8 Assay Result

Figure 6 shows CCK-8 assay result of the cells cultured on Ti disks, TiO₂ and ZrO₂ films for 1, 4, 7, and 10 days. At day 1, CCK-8 value on all surfaces appeared similar. After 4 and 7 days of incubation, cell proliferation on TiO₂ and ZrO₂ films was higher than that on Ti disks ($p < 0.05$). At day 10, there was no significant difference in cell proliferation on all the surfaces. No significant difference in cell proliferation was observed on ZrO₂ films when compared with TiO₂ films at each time point ($p > 0.05$).

3.4 ALP Activity

Figure 7 shows the ALP activity of MG63 cells on all the surfaces at various time points. At day 1, there was no significant difference in ALP activity on all the surfaces ($p > 0.05$). However, by days 4, 7 and 10, the ALP activity

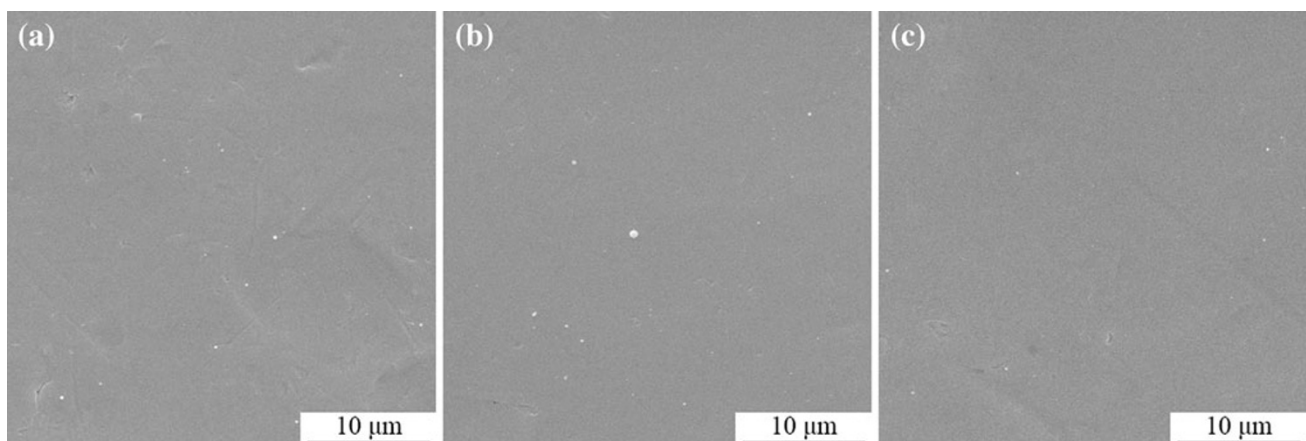


Fig. 1 Surface morphologies of the Ti disks (a), titania films (b) and zirconia films (c)

Fig. 2 Surface views of the TiO₂ and ZrO₂ films deposited on silicon wafers using filtered cathodic deposition obtained by AFM

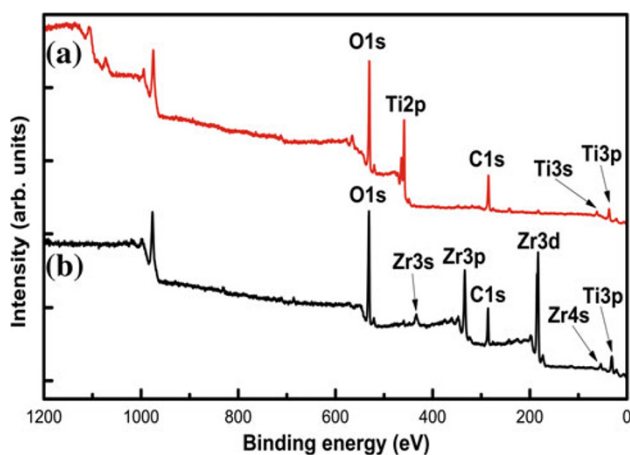
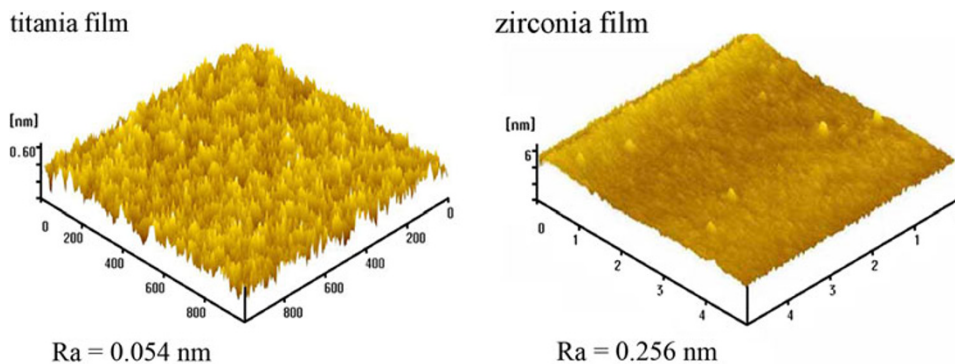


Fig. 3 Full range XPS spectra of titania film (a) and zirconia film (b)

was significantly higher on ZrO₂ films than that on Ti disks ($p < 0.05$). After 7 and 10 days of culture, the ALP activity showed significantly higher on TiO₂ films than on Ti disks ($p < 0.05$). The ALP activity on ZrO₂ films presented higher than on TiO₂ films at each time point, but statistically significant difference was only observed at day 4 ($p < 0.05$).

3.5 Fluorescence Microscopy of COLI

Figure 8 shows fluorescence microscopy of COLI in the cells cultured for 4 days. Osteoblasts cultured on ZrO₂ films (Fig. 7c) and TiO₂ films (Fig. 7b) produced more COLI than on Ti disks (Fig. 7a). No obvious difference in COLI production was observed between cells on TiO₂ and ZrO₂ films. Mean density of COLI immunofluorescence on TiO₂ and ZrO₂ films was significantly higher than on Ti disks ($p < 0.05$) (Fig. 7d).

3.6 Real-Time PCR Results

Figure 9 shows integrin β 1 (Fig. 9a), ERK1 (Fig. 9b), ERK2 (Fig. 9c) and *c-fos* (Fig. 9d) Quantitative PCR results of the MG63 cells cultured on all surfaces. After 6,

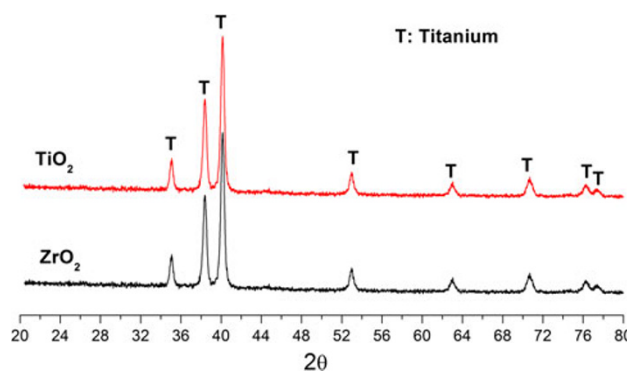


Fig. 4 Thin film XRD patterns of the TiO₂ and ZrO₂ films

24 h and 4 days of culture, integrin β 1 mRNA expression was significantly higher on ZrO₂ and TiO₂ films than on Ti disks ($p < 0.05$). At day 7, no statistically significant difference in integrin β 1 mRNA expression on all surfaces was observed ($p > 0.05$). Integrin β 1 mRNA expression on ZrO₂ films presented higher than on TiO₂ films at each time point, but the difference was not statistically significant ($p > 0.05$). After incubated for 6 and 24 h, ERK1 mRNA expression was significantly higher on ZrO₂ than on Ti disks ($p < 0.05$). At 6 h, ERK1 mRNA expression was significantly higher on TiO₂ films than on Ti disks ($p < 0.05$). At days 4 and 7, no significant difference in ERK1 gene expression was observed on all the surfaces ($p > 0.05$). After 6, 24 h and 4 days of incubation, ERK2 mRNA expression on ZrO₂ and TiO₂ films was significantly higher than on Ti disks ($p < 0.05$). At day 7, ERK2 mRNA expression showed no significant difference on all the surfaces ($p > 0.05$). There was no statistically significant difference in ERK2 mRNA expression level between ZrO₂ and TiO₂ films at each time point ($p > 0.05$). After cultured for 6, 24 h and 4 days, *c-fos* mRNA appeared significantly higher on ZrO₂ and TiO₂ films than on Ti disks ($p < 0.05$). At day 7, *c-fos* mRNA expression on ZrO₂ films was significantly higher than on Ti disks ($p < 0.05$). *c-fos* mRNA expression level showed no significant difference between ZrO₂ and TiO₂ films at each time point ($p > 0.05$).

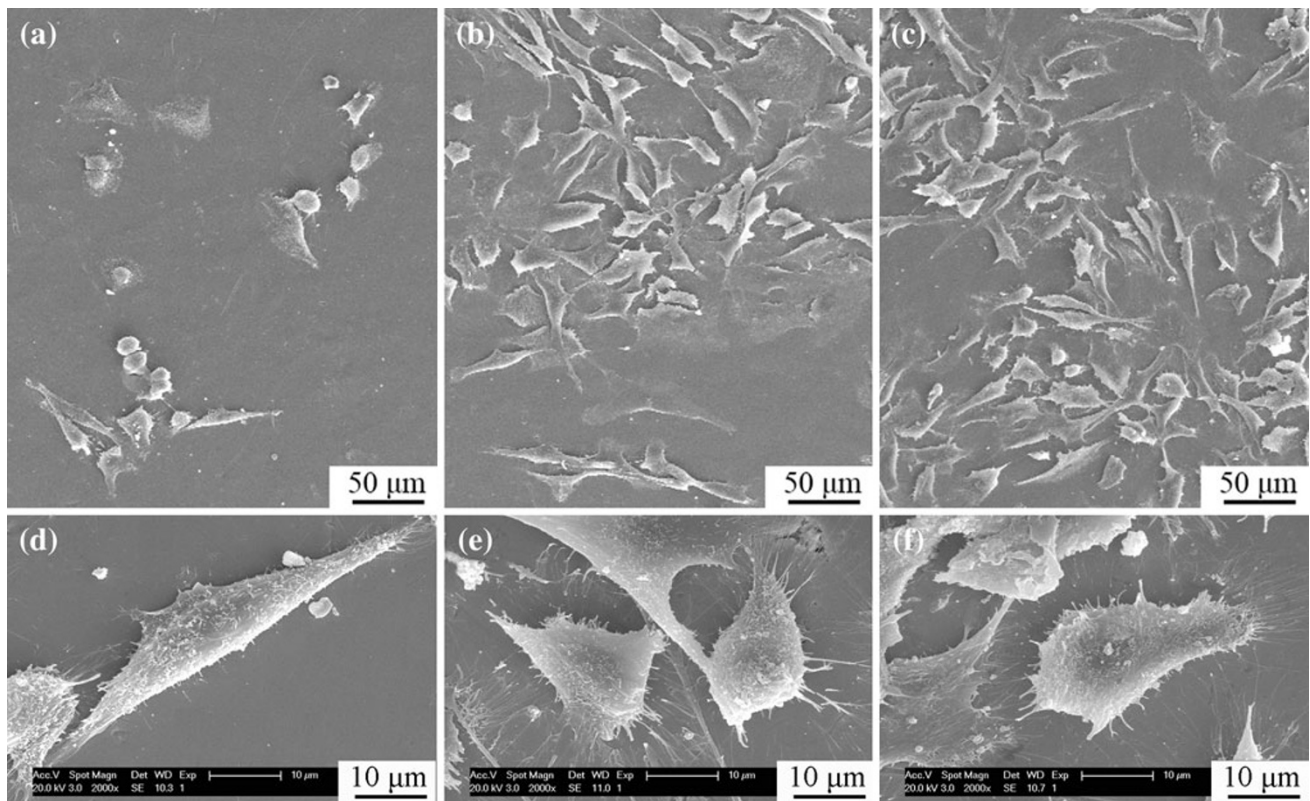


Fig. 5 Morphology of MG63 cells attached on titanium disks (a, d), titania films (b, e) and zirconia films (c, f) for 24 h at $\times 200$ magnification (a, b, c) ($bar = 50 \mu m$) and $\times 2,000$ magnification (d, e, f) ($bar = 10 \mu m$)

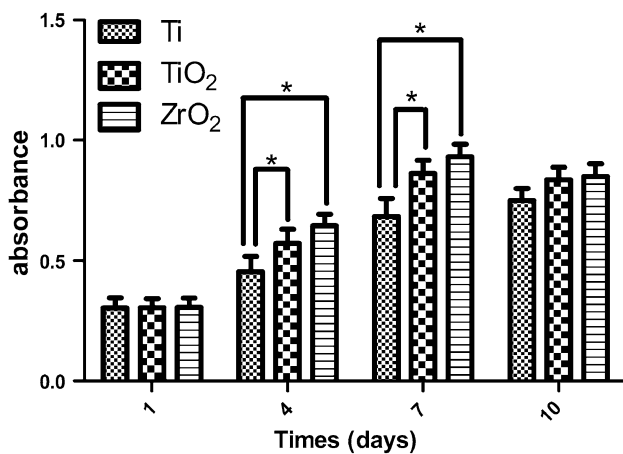


Fig. 6 CCK-8 result of MG63 cells cultured on Ti disks, titania films and zirconia films for 1, 4, 7, and 10 days. Asterisks show significance at $p < 0.05$

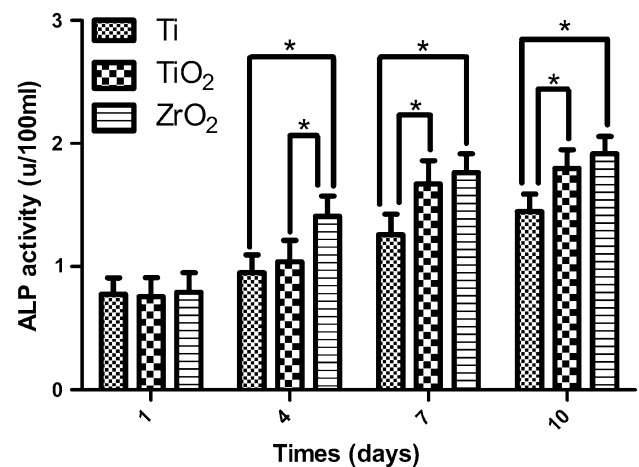


Fig. 7 ALP activity of MG63 cells cultured on Ti disks, titania films and zirconia films for 1, 4, 7, and 10 days. Asterisks show significance at $p < 0.05$

4 Discussion

The clinical success of an implant is strongly affected by osseointegration of the implant with juxtaposed bone which depends directly on the interactions between bone matrix and osteoblasts with the biomaterial. The surface characteristics of the implant material have important

effects in determining bone adaptation to the implant. In this work, we deposited amorphous TiO₂ films and ZrO₂ films on Ti disks respectively by cathodic arc deposition. Then we evaluated the adhesion, proliferation and differentiation of MG63 osteoblastic cells on Ti disks, TiO₂ films, and ZrO₂ films and studied possible molecular

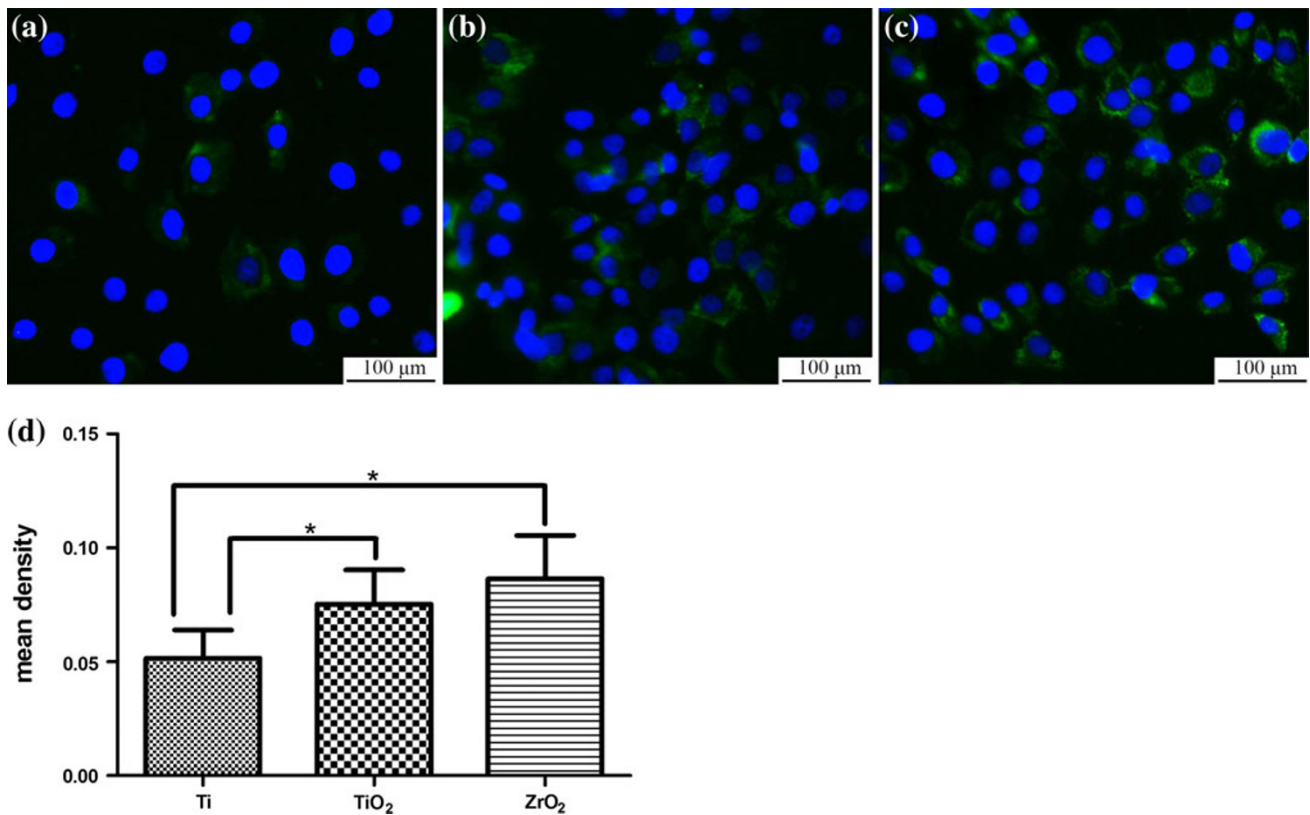
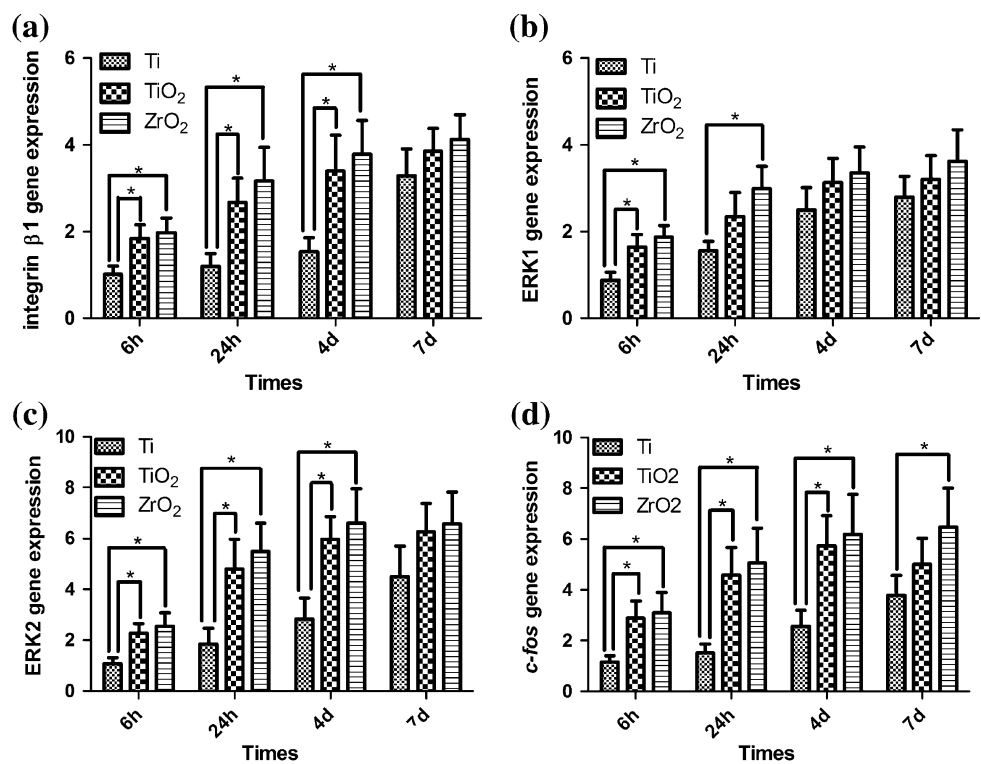


Fig. 8 Immunofluorescence labeling of COLI (green) and Nucleus (blue) of MG63 cells cultured on Ti disks (a), titania films (b) and zirconia films (c) for 4 days (bar = 100 μm) and mean density of COLI immunofluorescence analyzed by IPP (d). Asterisks show significance at $p < 0.05$

Fig. 9 Integrin β1 (a), ERK1 (b), ERK2 (c) and c-fos (d) mRNA expression of MG63 cells cultured on Ti disks, titania films and zirconia films for 6, 24 h and 4, 7 days. Asterisks show significance at $p < 0.05$



mechanism that would affect the biological behavior of the cells.

The first phase of cell-material interaction involves cell adhesion and spreading. This first phase controls the subsequent cell–matrix interaction and cell differentiation upon contact with the implant [26, 27]. SEM observations from our work showed that the attachment and spreading of MG63 cells on ZrO₂ and TiO₂ films are more pronounced than those on Ti disks after 24 h of culture and filopodia extensions from the cells to the substrate are more abundant on ZrO₂ and TiO₂ films than on Ti disks. These results suggest that both ZrO₂ films and TiO₂ films are more preferential for cell attachment and spreading behavior than Ti disks.

Osteoblast proliferation plays an important role in the process of new bone formation. CCK-8 assay reflects the cell metabolic activity, which is linked with cell proliferation during the exponential phase of growth in vitro. Our study indicates that cell proliferation appeared higher at early time points on ZrO₂ films and TiO₂ films than on Ti disks.

ALP has been widely recognized as an important early marker for osteoblast differentiation [28]. The level of ALP activity is an indicator of osteoblast differentiation [29, 30]. Our results showed that ALP activity of MG63 cells on ZrO₂ and TiO₂ films is higher than on Ti disks at day 4, 7 and 10, which reflected more rapid induction of osteoblastic phenotype of MG63 cells on ZrO₂ and TiO₂ films. Higher ALP activity on ZrO₂ films than on TiO₂ films at day 4 indicates that the amorphous ZrO₂ films may lead to promotion of a more osteoblastic phenotype of MG-63 cells than TiO₂ films and further study is needed to testify this.

Furthermore, we investigated the production of COLI by fluorescence immunostaining. COLI is an important marker of the osteoblastic differentiation. In this study, osteoblasts on ZrO₂ and TiO₂ films produced more COLI compared to Ti disks at day 4, indicating promotion of a more osteoblastic phenotype of MG-63 cells on ZrO₂ and TiO₂ films. COLI is a molecule of extracellular matrix and can be secreted by osteoblast. In general, osteoblasts synthesize procollagen inside the cells during early culture stage. After cultured for 10–12 days, plenty of collagen is secreted to extracellular matrix. In our work, the cells were cultured for 4 days and the COLI was found inside the cells. The reason that the collagen was not secreted may be the culture time is too short.

Osteoblasts interact with their substrate initially via integrins binding to proteins adsorbed on the surface of a biomaterial and later, to proteins in their secreted ECM. When an implant is placed in a defect or in culture medium, proteins such as vitronectin or fibronectin will adsorb to the surface of the implant material [31]. Integrins then

bind to these ECM proteins and become cluster in the plane of the cell membrane. After clustering, various protein tyrosine kinases, including focal adhesion kinase (FAK), Src family kinases, are activated. Finally, cytoskeleton and multiple signaling molecules will be recruited and activated [32], leading to promotion of the actin filaments assembly and stimulation of the mitogen activated protein kinase (MAPK) pathway [23]. Among the integrin family, integrin $\beta 1$ seems to be one of the main cell surface receptors to interact with ECM molecules or scaffolds [26, 33, 34].

Surface properties of the substrate can influence protein adsorption and integrin expression on a biomaterial [32, 35], resulting in different signaling pathways. Finally, the difference will affect the regulation of cell adhesion, motility, proliferation, and differentiation [36, 37].

ERK1 and ERK2 are two isoforms of MAP kinase superfamily and are not only essential for osteoblast growth and differentiation, but also important for osteoblast adhesion, spreading, migration, and integrin expression [38, 39]. Activated ERK1 and ERK2 translocate to the nucleus and phosphorylate the activator protein-1(AP-1) transcription factors. *c-fos*, a member of the AP-1 transcription factor complex, is associated with bone cell's growth and differentiation and has much effect on osteoblasts and osteoclasts during the normal development and bone diseases [40, 41]. Our results demonstrated that integrin $\beta 1$, ERK1, ERK2 and *c-fos* gene expression was enhanced in cells cultured on TiO₂ and ZrO₂ films at early time points of culture. This is in agreement with the findings of Zreiqat et al. [42], who found that human bone-derived cells (HBDC) can bind directly to the implant surface and integrin $\beta 1$ expression was modulated as a result of magnesium ions modification of the underlying bioceramic substrata. Zreiqat et al. [43] also found that modifying Ti-6Al-4V with CHAP or Mg upregulated integrin $\beta 1$, ERK and *c-fos* expression of HBDC which may potentially contribute to successful osteoblast function and differentiation.

Gene expression is not equal to cell signaling and activation of the ERK/MAPK pathway is characterized by the phosphorylation and not the up-regulation of their own gene expression. But difference in gene expression of signaling molecules can to some extent partially reflect the change in signaling transduction and has been used to study the signaling transduction pathways in previous work [24]. Our results indicate that the change in integrin $\beta 1$, ERK and *c-fos* gene expression in cells on TiO₂ and ZrO₂ films may potentially have an effect on the biological behavior of MG-63 cells. There may be other signaling pathways can regulate the ERK1/2 gene expression, and this pathway has other more prominent target genes. Our present work is a preliminary research to test the hypothesis that that the

ZrO₂ films and TiO₂ films may promote osteogenesis partially through integrin β 1 mediated MAPK signaling pathway. We will investigate the induction of different signaling pathways by investigation of the phosphorylation in our further study.

The finding that integrin β 1 gene expression is up-regulated in better adhering cells is in contrast to other literature [44], which describes that integrins are up-regulated in non-adherent MG63 cells. Differences between studies in integrin expression may be the result of cell source, or in vivo versus in vitro characterization. There are also technical reasons for differences, including the detection technique, method for fixation and permeabilization, antibody specificity, and immunostaining conditions [32].

The enhanced biological behavior of osteoblasts on ZrO₂ films may be due to the surface properties of the amorphous ZrO₂ films. The surface charge of the ZrO₂ is generally regarded to be negative [22, 45]. Filtered cathodic arc deposition is a very efficient method for producing nanostructured films and the AFM result indicated that the TiO₂ and ZrO₂ films deposited by filtered cathodic arc deposition have a nanostructured surface. Previous research has found finer nano-crystalline particles have higher surface charge densities than larger ones [46]. Thus, the nanostructured surface of the amorphous ZrO₂ film may have higher negative surface charge. Proteins that have a number of positively/negatively charged residues are expected to show a high affinity for the negatively/positively charged surface of a material. Han et al. [47] found that negatively charged TiO₂ coating has beneficial effect on cell adhesion, proliferation and differentiation. Zhang et al. [48] also found that negatively charged phosphate groups developed on zirconia surface by hydrothermal treatment in phosphoric solutions could enhance marrow cell response. Therefore, in this work, the nanostructured surface of the amorphous ZrO₂ film may be the key factor to promote the adhesion, proliferation and differentiation of osteoblasts.

5 Conclusions

Amorphous TiO₂ and ZrO₂ films were deposited on Ti disks respectively by cathodic arc deposition. Both the TiO₂ and ZrO₂ films could not only stimulate the adhesion, proliferation of MG-63 cells, but also enhance induction of osteoblastic phenotype of MG-63 cells. In addition, the ALP activity of MG63 cells on ZrO₂ films was higher than on TiO₂ films at day 4, which indicate that ZrO₂ films may promote more osteoblastic phenotype of MG-63 cells than TiO₂ films. Moreover, the TiO₂ films and ZrO₂ films could both increase integrin β 1, ERK1/2, and *c-fos* gene expression. These results suggest that the amorphous ZrO₂

film produced by cathodic arc deposition may be a promising biomaterial that can enhance adhesion, proliferation and differentiation of osteoblasts in vitro and worth further study.

Acknowledgments This work was jointly supported by National Basic Research Program of China (973 Program, 2012CB933601), National Natural Science Foundation of China (30973041, 31100675 and 51071168), Shanghai Science and Technology R&D Fund (11JC1413700), Research and Innovation Project for College Graduates of Jiangsu Province (CXLX12_0844).

Open Access This article is distributed under the terms of the Creative Commons Attribution License which permits any use, distribution, and reproduction in any medium, provided the original author(s) and the source are credited.

References

- Simon M, Lagneau C, Moreno J, Lissac M, Dalard F, Grosogeat B (2005) *Eur J Oral Sci* 113(6):537–545. doi:10.1111/j.1600-0722.2005.00247.x
- Chiesa R, Giavaresi G, Fini M, Sandrini E, Giordano C, Bianchi A, Giardino R (2007) *Oral Surg Oral Med Oral Pathol Oral Radiol Endod* 103(6):745–756. doi:10.1016/j.tripleo.2006.09.025
- Le Guehenec L, Soueidan A, Layrolle P, Amouriq Y (2007) *Dent Mater* 23(7):844–854. doi:10.1016/j.dental.2006.06.025
- Cooper LF, Zhou Y, Takebe J, Guo J, Abron A, Holmen A, Ellingsen JE (2006) *Biomaterials* 27(6):926–936. doi:10.1016/j.biomaterials.2005.07.009
- Guo J, Padilla RJ, Ambrose W, De Kok JJ, Cooper LF (2007) *Biomaterials* 28(36):5418–5425. doi:10.1016/j.biomaterials.2007.08.032
- Park JW, Park KB, Suh JY (2007) *Biomaterials* 28(22):3306–3313. doi:10.1016/j.biomaterials.2007.04.007
- Park JW, Jang JH, Lee CS, Hanawa T (2009) *Acta Biomater* 5(6):2311–2321. doi:10.1016/j.actbio.2009.02.026
- Sul YT, Johansson C, Byon E, Albrektsson T (2005) *Biomaterials* 26(33):6720–6730. doi:10.1016/j.biomaterials.2005.04.058
- Anders A (1997) *Surf Coat Tech* 93(2–3):158–167. doi:10.1016/S0257-8972(97)00037-6
- Vyskocil J, Musil J (1992) *J Vac Sci Technol A Vac Surf Films* 10(4):1740–1748
- Ostrikov K (2005) *Rev Mod Phys* 77(2):489–511. doi:10.1103/RevModPhys.77.489
- Li WF, Liu XY, Huang AP, Chu PK (2007) *J Phys D-Appl Phys* 40(8):2293–2299. doi:10.1088/0022-3727/40/8/s08
- Xiao F, Tsuru K, Hayakawa S, Osaka A (2003) *Thin Solid Films* 441(1–2):271–276. doi:10.1016/S0040-6090(03)00913-1
- Yang BC, Uchida M, Kim HM, Zhang XD, Kokubo T (2004) *Biomaterials* 25(6):1003–1010. doi:10.1016/S0142-9612(03)00626-4
- Zhou W, Zhong X, Wu X, Yuan L, Shu Q, Xia Y, Ken Ostrikov K (2007) *J Biomed Mater Res, Part A* 81A(2):453–464. doi:10.1002/jbm.a.30987
- Kokubo T, Kim HM, Kawashita M (2003) *Biomaterials* 24(13):2161–2175. doi:10.1016/S0142-9612(03)00044-9
- Liu X, Zhao X, Li B, Cao C, Dong Y, Ding C, Chu PK (2008) *Acta Biomater* 4(3):544–552. doi:10.1016/j.actbio.2008.01.011
- Amin MS, Randeniya LK, Bendavid A, Martin PJ, Preston EW (2010) *Thin Solid Films* 519(4):1300–1306. doi:10.1016/j.tsf.2010.09.029

19. Yan YY, Han Y (2007) *Surf Coat Tech* 201(9–11):5692–5695. doi:[10.1016/j.surfcoat.2006.07.058](https://doi.org/10.1016/j.surfcoat.2006.07.058)
20. Wang G, Meng F, Ding C, Chu PK, Liu X (2010) *Acta Biomater* 6(3):990–1000. doi:[10.1016/j.actbio.2009.09.021](https://doi.org/10.1016/j.actbio.2009.09.021)
21. Sollazzo V, Pezzetti F, Scarano A, Piattelli A, Bignozzi CA, Massari L, Brunelli G, Carinci F (2008) *Dent Mater* 24(3):357–361. doi:[10.1016/j.dental.2007.06.003](https://doi.org/10.1016/j.dental.2007.06.003)
22. Liu XY, Huang AP, Ding CX, Chu PK (2006) *Biomaterials* 27(21):3904–3911. doi:[10.1016/j.biomaterials.2006.03.007](https://doi.org/10.1016/j.biomaterials.2006.03.007)
23. Giancotti FG, Ruoslahti E (1999) *Science* 285(5430):1028–1032. doi:[10.1126/science.285.5430.1028](https://doi.org/10.1126/science.285.5430.1028)
24. Au AY, Au RY, Demko JL, McLaughlin RM, Eves BE, Frondoza CG (2010) *J Biomed Mater Res A* 94(2):380–388. doi:[10.1002/jbm.a.32668](https://doi.org/10.1002/jbm.a.32668)
25. Cheng SL, Lai CF, Blystone SD, Avioli LV (2001) *J Bone Miner Res* 16(2):277–288. doi:[10.1359/jbmr.2001.16.2.277](https://doi.org/10.1359/jbmr.2001.16.2.277)
26. Anselme K (2000) *Biomaterials* 21(7):667–681. doi:[10.1016/S0142-9612\(99\)00242-2](https://doi.org/10.1016/S0142-9612(99)00242-2)
27. Saldana L, Vilaboa N (2010) *Acta Biomater* 6(4):1649–1660. doi:[10.1016/j.actbio.2009.10.033](https://doi.org/10.1016/j.actbio.2009.10.033)
28. Li D, Dai K, Tang T (2008) *Cytotherapy* 10(6):587–596. doi:[10.1080/14653240802238330](https://doi.org/10.1080/14653240802238330)
29. Cowles EA, DeRome ME, Pastizzo G, Brailey LL, Gronowicz GA (1998) *Calcif Tissue Int* 62(1):74–82. doi:[10.1007/s002239900397](https://doi.org/10.1007/s002239900397)
30. Whyte MP (1994) *Endocr Rev* 15(4):439–461. doi:[10.1210/edrv-15-4-439](https://doi.org/10.1210/edrv-15-4-439)
31. Wilson CJ, Clegg RE, Leavesley DI, Pearcy MJ (2005) *Tissue Eng* 11(1–2):1–18. doi:[10.1089/ten.2005.11.1](https://doi.org/10.1089/ten.2005.11.1)
32. Siebers MC, ter Brugge PJ, Walboomers XF, Jansen JA (2005) *Biomaterials* 26(2):137–146. doi:[10.1016/j.biomaterials.2004.02.021](https://doi.org/10.1016/j.biomaterials.2004.02.021)
33. Lee M, Lee HJ, Seo WD, Park KH, Lee YS (2010) *Int J Radiat Oncol Biol Phys* 76(5):1528–1536. doi:[10.1016/j.ijrobp.2009.11.022](https://doi.org/10.1016/j.ijrobp.2009.11.022)
34. Lu ZF, Zreiqat H (2010) *Biochem Biophys Res Commun* 394(2):323–329. doi:[10.1016/j.bbrc.2010.02.178](https://doi.org/10.1016/j.bbrc.2010.02.178)
35. Sinha RK, Tuan RS (1996) *Bone* 18(5):451–457. doi:[10.1016/8756-3282\(96\)00044-0](https://doi.org/10.1016/8756-3282(96)00044-0)
36. Stephansson SN, Byers BA, Garcia AJ (2002) *Biomaterials* 23(12):2527–2534. doi:[10.1016/S0142-9612\(01\)00387-8](https://doi.org/10.1016/S0142-9612(01)00387-8)
37. Olivares-Navarrete R, Raz P, Zhao G, Chen J, Wieland M, Cochran DL, Chaudhri RA, Ornoy A, Boyan BD, Schwartz Z (2008) *Proc Natl Acad Sci U S A* 105(41):15767–15772. doi:[10.1073/pnas.0805420105](https://doi.org/10.1073/pnas.0805420105)
38. Lai CF, Chaudhary L, Fausto A, Halstead LR, Ory DS, Avioli LV, Cheng SL (2001) *J Biol Chem* 276(17):14443–14450. doi:[10.1074/jbc.M010021200](https://doi.org/10.1074/jbc.M010021200)
39. Krause A, Cowles EA, Gronowicz G (2000) *J Biomed Mater Res* 52(4):738–747. doi:[10.1002/1097-4636\(20001215\)52:4<738::AID-JBM19>3.0.CO;2-F](https://doi.org/10.1002/1097-4636(20001215)52:4<738::AID-JBM19>3.0.CO;2-F)
40. Machwate M, Jullienne A, Moukhtar M, Marie PJ (1995) *J Cell Biochem* 57(1):62–70. doi:[10.1002/jcb.240570108](https://doi.org/10.1002/jcb.240570108)
41. Papachristou DJ, Batistatou A, Sykiotis GP, Varakis I, Papavassiliou AG (2003) *Bone* 32(4):364–371. doi:[10.1016/S8756-3282\(03\)00026-7](https://doi.org/10.1016/S8756-3282(03)00026-7)
42. Zreiqat H, Howlett CR, Zannettino A, Evans P, Schulze-Tanzil G, Knabe C, Shakibaei M (2002) *J Biomed Mater Res* 62(2):175–184. doi:[10.1002/jbm.10270](https://doi.org/10.1002/jbm.10270)
43. Zreiqat H, Valenzuela SM, Nissan BB, Roest R, Knabe C, Radlanski RJ, Renz H, Evans PJ (2005) *Biomaterials* 26(36):7579–7586. doi:[10.1016/j.biomaterials.2005.05.024](https://doi.org/10.1016/j.biomaterials.2005.05.024)
44. Chen D, Magnuson V, Hill S, Arnaud C, Steffensen B, Klebe RJ (1992) *J Biol Chem* 267(33):23502–23506
45. Moritz T, Benfer S, Arki P, Tomandl G (2001) *Sep Purif Technol* 25(1–3):501–508. doi:[10.1016/S1383-5866\(01\)00080-6](https://doi.org/10.1016/S1383-5866(01)00080-6)
46. Vayssieres L, Chaneac C, Tronc E, Jolivet JP (1998) *J Colloid Interface Sci* 205(2):205–212. doi:[10.1006/jcis.1998.5614](https://doi.org/10.1006/jcis.1998.5614)
47. Han Y, Chen D, Sun J, Zhang Y, Xu K (2008) *Acta Biomater* 4(5):1518–1529. doi:[10.1016/j.actbio.2008.03.005](https://doi.org/10.1016/j.actbio.2008.03.005)
48. Zhang J, Jiang D, Kotobuki N, Maeda M, Hirose M, Ohgushi H (2006) *Appl Phys Lett* 89 (18). doi:[10.1063/1.2385208](https://doi.org/10.1063/1.2385208)